Lawrence Berkeley Laboratory
UNIVERSITY OF CALIFORNIA

Presented at the International Conference on New
Nuclear Physics with Advanced Techniques,
Ierapetra, Crete, June 23–29, 1991, and
to be published in the Proceedings

Studies of Multifragment Decay in Reverse Kinematics

L.G. Moretto, P. Roussel-Chomaz, M. Colonna,
N. Colonna, and G.J. Wozniak

June 1991

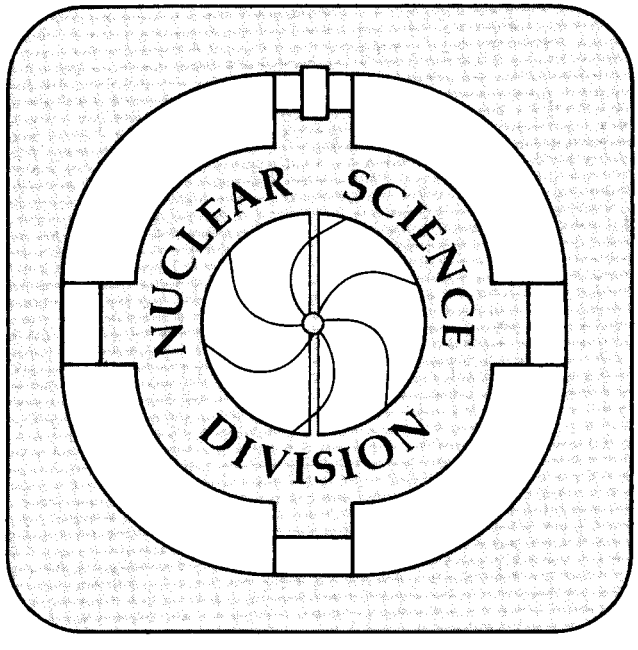

Prepared for the U.S. Department of Energy under Contract Number DE-AC03-76SF00098

DISCLAIMER

LBL-30929

Studies of Multifragment Decay in Reverse Kinematics

L.G. Moretto, P. Roussel-Chomaz, M. Colonna,
N. Colonna, and G.J. Wozniak

Nuclear Science Division
Lawrence Berkeley Laboratory
University of California
Berkeley, CA 94720

June 1991

This work was supported by the Director, Office of Energy Research, Office of High Energy and Nuclear Physics, Division of Nuclear Physics, of the U.S. Department of Energy under Contract No. DE-AC03-76SF00098

Studies of Multifragment Decay in Reverse Kinematics

L.G. Moretto, P. Roussel-Chomaz[a)], M. Colonna[b)], N. Colonna, and G.J. Wozniak

Nuclear Science Division, Lawrence Berkeley Laboratory

1 Cyclotron Road, Berkeley, CA 94720

Abstract

Multifragment events are shown to be associated with specific sources characterized by their mass and excitation energy through the incomplete fusion model. Excitation functions for the different multifragment decay channels are found to be almost independent of the system and the incident energy. Preliminary comparisons of the data with dynamical calculations followed by statistical decay calculations are discussed.

Introduction

Within the incomplete fusion picture, it is possible to correlate the mass and excitation energy of the product nucleus with the degree of fusion by means of the source velocity. In reverse kinematics, for large impact parameters the nuclei formed are slightly heavier than the projectile and move at slightly lower velocity. As the impact parameter decreases, the projectile picks up more and more mass from the target, the velocity of the compound system decreases and its excitation energy increases. This correlation, clearly observed for the 18 MeV/u ^{139}La + ^{64}Ni reaction[1], made it possible to study, at one incident energy, the decay properties of hot nuclei over a large excitation energy range.

We have extended this method to ternary, quaternary, etc... events[2]. We have also compared our experimental results to some very preliminary results[3] obtained by coupling a Landau-Vlasov type calculation [4] describing the dynamical stage of the collision with a statistical binary decay code[5, 6] used to describe the deexcitation process. These results may help us to understand the role played by the dynamics and by the statistics in these collisions.

Experimental results

Multifragment emission has been studied in the reactions induced by ^{139}La beams on different targets: ^{12}C,^{27}Al,^{40}Ca,^{51}V,^{nat}Cu, and ^{139}La[1-3]. Because of the reverse kinematics, even the heaviest fragments have velocities large enough to be identified easily with simple ΔE-E telescopes. Furthermore the reaction products are focused in a narrow cone around the beam direction; therefore the detection efficiency is good even with a detection system of modest size.

Fig. 1 presents, for the 2-body events, the correlation between the source velocities (normalized to the beam velocity), and the total charge detected, for six different energies ranging from 18 to 55 MeV/u and four entrance channel asymmetries.

---

a) Permanent address: CEN Saclay, 91191 Gif sur Yvette Cedex France

b) Present address: Universita di Catania, 95129 Catania, Italy

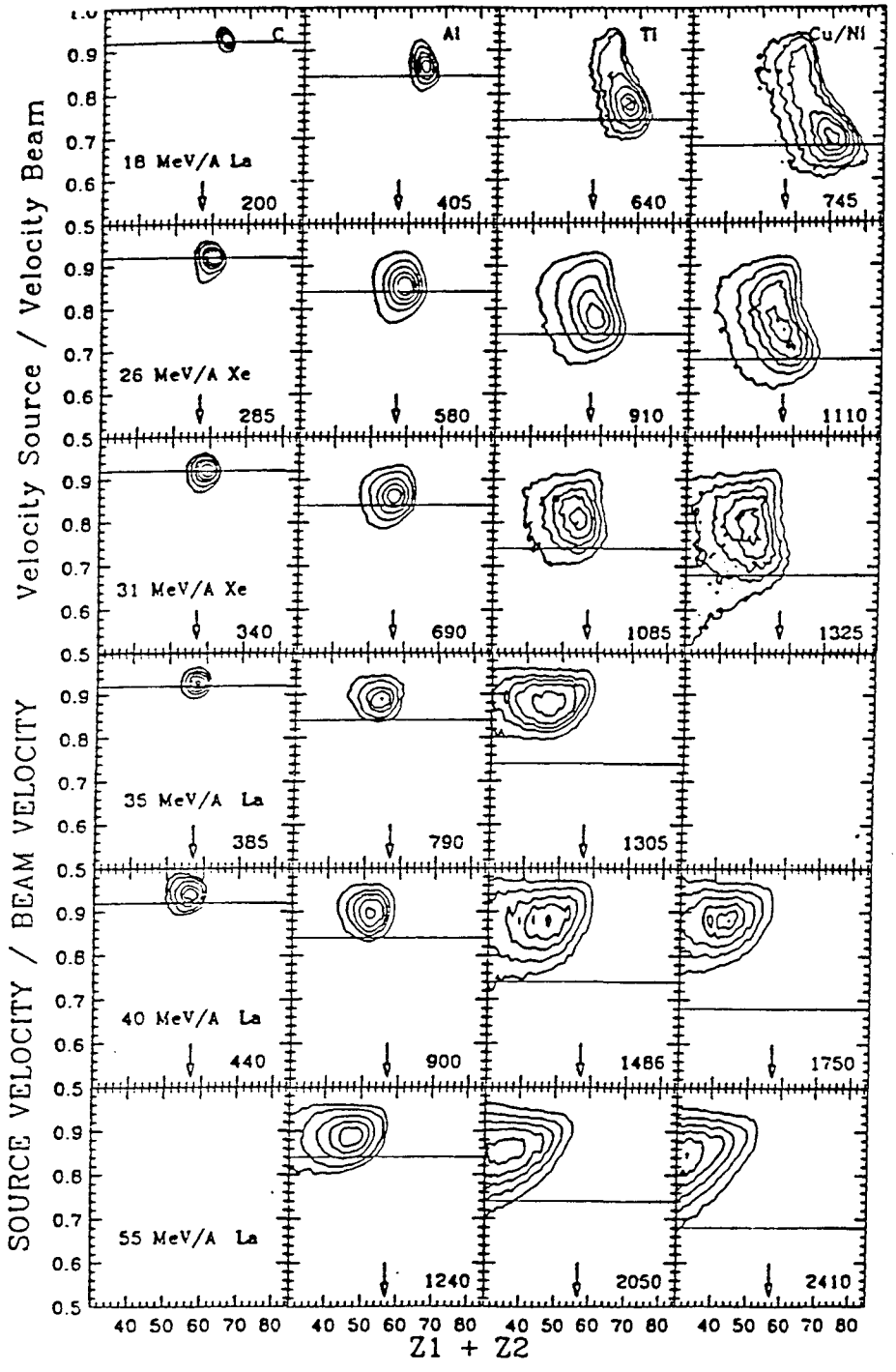

Fig. 1: Linear contour plots of the source velocity versus total detected charge for 2-fold coincidence events, for 6 incident energies and 4 different entrance channel asymmetries. The beam energy and the target are indicated in the first row and column, respectively. The total available energy in the c.m. system is indicated in the lower right of each frame. The horizontal lines and the vertical arrows indicate the complete fusion velocity for each system and the projectile charge, respectively. The data corresponding to ^{129}Xe beams have been shifted by 3 Z-units to make the comparison easier ($\Delta Z_{La-Xe}=3$).

The first row corresponds to the most asymmetric system La/Xe + ^{12}C, which has relatively low available energies in the center of mass system, and presents a very simple pattern. At 18 MeV/u, the source velocity distribution peaks at the value expected for complete fusion, which corresponds to the solid line, and the total charge detected is the total charge of the system. In this case, complete fusion has occurred and only neutrons have been evaporated. When the incident energy increases, the distributions move to higher source velocities and lower total detected charge. The same description holds for the ^{27}Al target. The only difference is that, due to the higher excitation energies that can be reached, the evaporation is more extensive and the detected charge is less than that of the primary compound nucleus, even at 18 MeV/u.

The pattern observed for the heavier targets is more complicated. At 18 MeV/u we observe a very nice illustration of the transition from complete fusion ($Z_1+Z_2 \approx Z_P+Z_T$) to incomplete fusion, with a ridge line going to lower secondary charge when the source velocity increases, which is again what is expected for incomplete fusion in reverse kinematics. As the incident energy increases, and the excitation energy available in the reaction increases, the pattern shifts towards lower Z values because of the evaporation process. At 35 MeV/u the pattern observed is upright, indicating that the system has lost by evaporation as many nucleons as it had gained from the fusion with the target. The patterns observed for ^{51}V and ^{nat}Cu above 35 Mev/u are quite different, with a ridge line going to

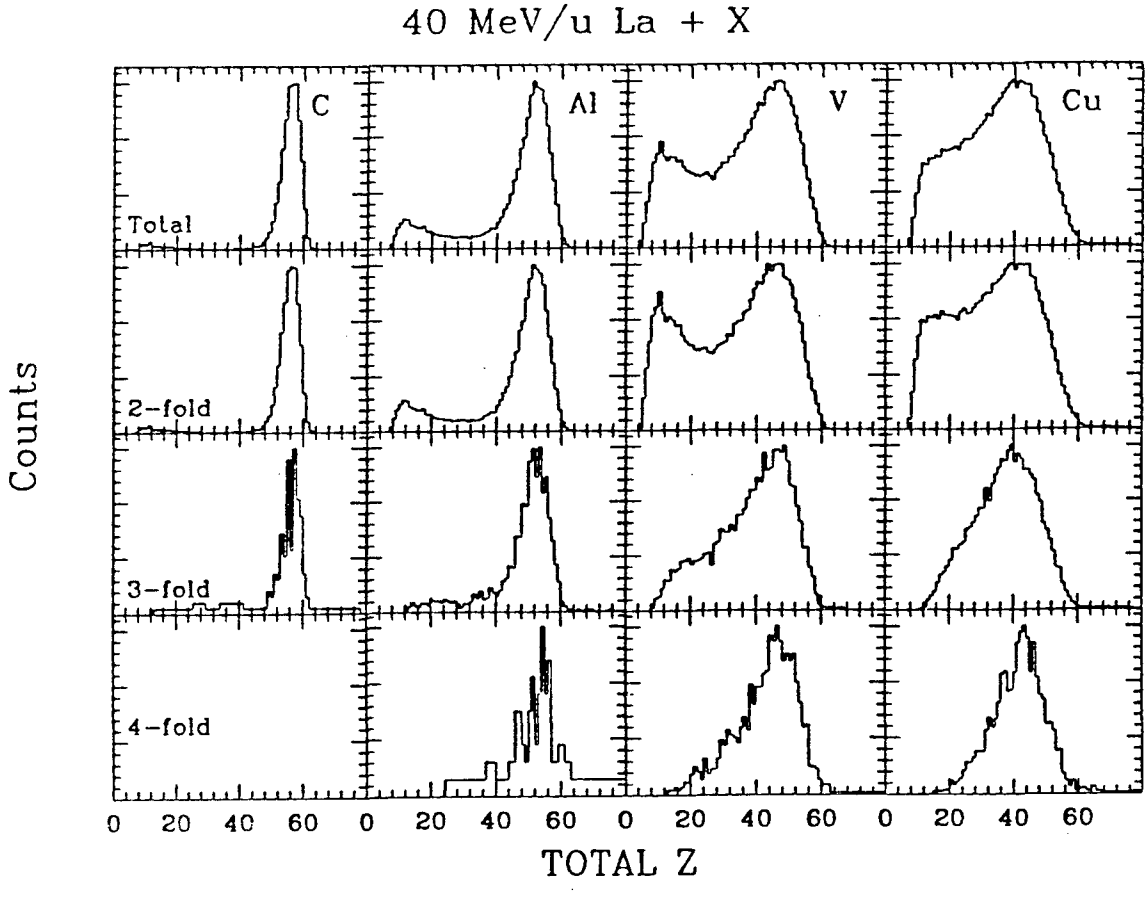

Fig. 2. Total detected charge for some of the systems measured at 40 MeV/u as a function of multiplicity in the exit channel.

lower secondary detected charge when the source velocity decreases, which is the opposite to what was observed at lower incident energy.

We shall now consider n-fold events, i.e. events where n fragments are detected in coincidence, with n = 2, 3, 4 and even 5 at 55 MeV/u. Fig. 2 presents the Z distributions for n-fold events for all the systems measured at 40 MeV/u. For the ^{12}C target a narrow peak is observed, but as the mass of target increases, this peak broadens and shifts to lower detected charge. These effects arise from the larger range of mass transfers and from the increase of light particle evaporation due to the larger range of excitation energies available. The tail at low total detected charges also increases with the mass of the target, and this is related to the increase of higher n-fold events where only 2 fragments are detected. The same Z_{total} distribution plotted for 3-fold and 4-fold events presents a peak centered at approximately the same value, but with a reduced tail to low Z_{total}, indicating that most of these events are complete.

In the following we will restrict ourselves to events where the total measured charge is higher than 30, in order to exclude those events where one fragment is clearly missing and to avoid biasing our kinematical reconstructions. Fig. 3 presents the source velocity distributions obtained at 40 MeV/u for all the targets and for the different fragment multiplicities. The observed peak broadens significantly when the mass of the target increases. This width has two different origins: incomplete fusion processes and the

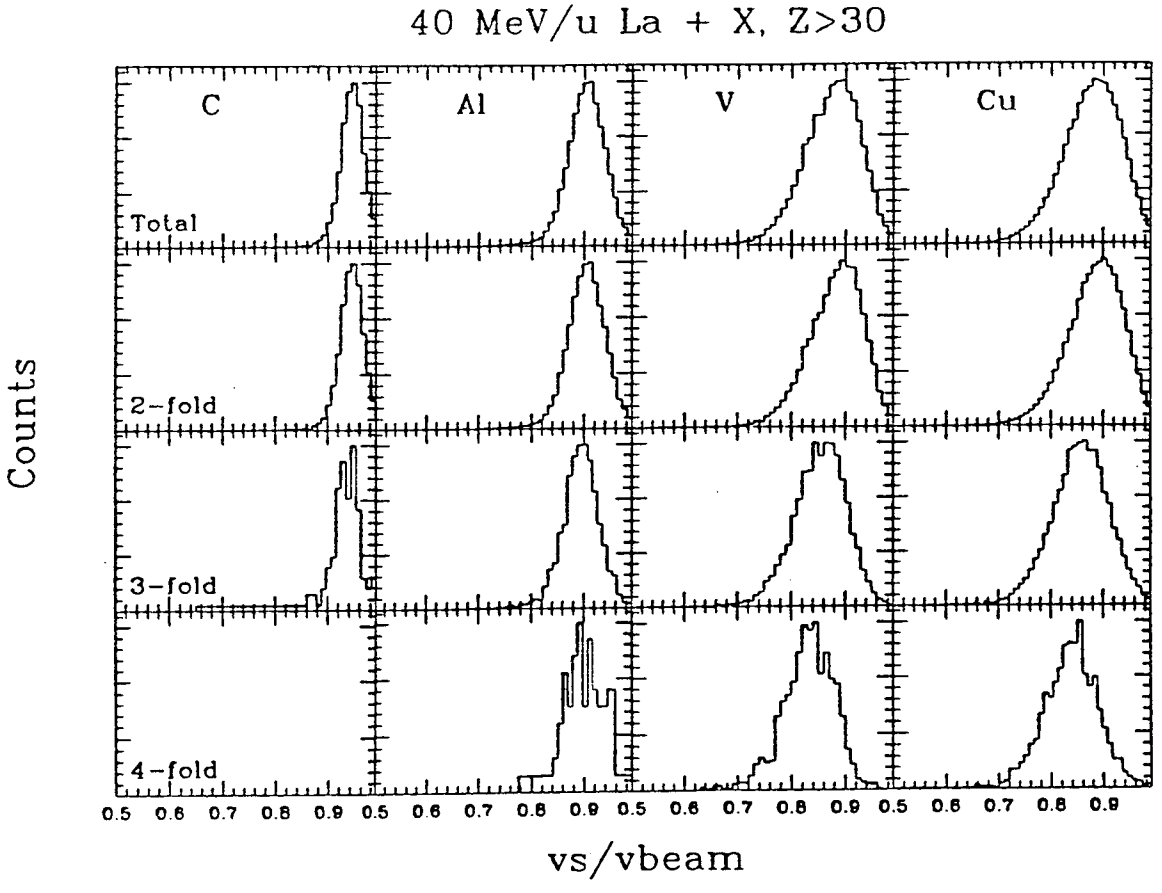

Fig. 3: Same as Fig. 2 for the source velocities expressed as the ratio of the source to the beam velocity.

broadening from evaporation. This contribution has been estimated with the statistical code Gemini[4, 5]. In the case of the ^{12}C target, the width can be explained almost entirely by light particle evaporation, but in the case of the heavier targets, a wide range of excitation energies contributes effectively to complex fragment emission. For a given target, the requirement of larger multiplicity of complex fragments selects out events with lower source velocities and therefore higher excitation energies. The same trend has been observed with Ne+Au at 60 MeV/u [7].

To study the behavior of hot nuclear systems as their excitation energy increases, excitation functions for the binary, ternary, etc. decay channels have been constructed. More precisely, Fig. 4 presents the evolution of the proportion of n-fold events with respect to the total number of coincidence events as a function of the excitation energy inferred from the source velocity through the incomplete fusion model, for four incident energies.

The picture obtained is quite striking. First, at all energies the 3-fold and 4-fold event probabilities (and 5-fold at 55 MeV/u) increase significantly up to excitation energies as high as 8 MeV/u. This energy dependence is a good indication that the relation between E^* and the source velocity is valid and also confirms that the width of the source velocity distribution is only partly due to light particle evaporation (if it were only particle evaporation, the excitation functions would be flat). Second, the increase observed in these excitation functions is essentially the same, for all systems, and at all bombarding energies,

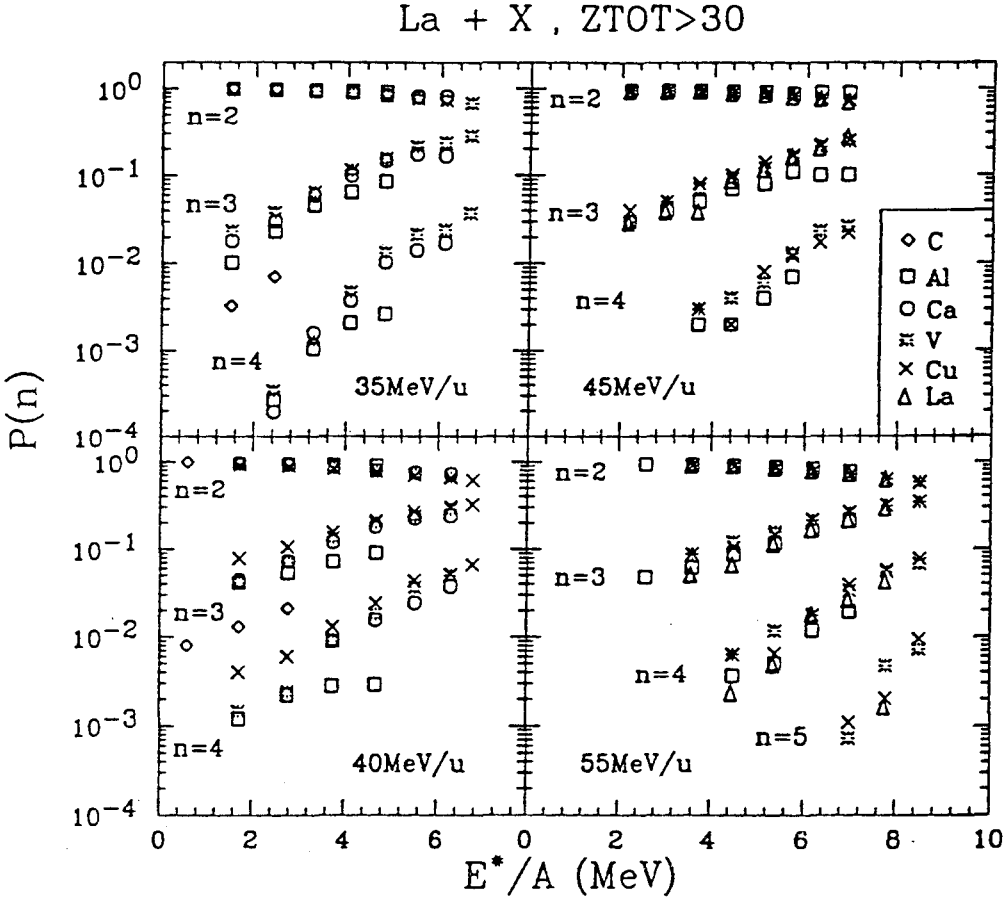

Fig. 4: Proportion of 2-3-4-5 fold events as a function of the excitation energy per nucleon for the systems studied at 4 different energies.

suggesting that the branching ratios for binary, ternary, quaternary decays depend mainly upon excitation energy (and angular momentum) and not upon the dynamics of the reaction.

To conclude on these excitation functions, their independence with respect to target-projectile combination and to incident energy suggests a competition between the different decay channels independent of the entrance channel and therefore supports the idea of an intermediate system whose decay properties are mainly determined by its excitation energy and angular momentum.

Boltzmann-Nordheim-Vlasov calculations

Kinetic equations, like the Landau-Vlasov, Boltzmann-Uehling-Uhlenbeck or Boltzmann-Nordheim-Vlasov equations, have been widely used to simulate the evolution of heavy-ion collisions in the intermediate energy range[8-13]. So far, these transport theories have not been able to reproduce the yields of fragments in the mass range between the projectile and target[13]. On the other hand, statistical approaches, where complex fragments are assumed to be produced in the decay of compound nuclei formed in fusion or incomplete fusion reactions, take minimal account of entrance channel effects and cannot reproduce the non-equilibrium features observed at intermediate energy[14].

The two approaches described above are complementary and can be combined in a framework which incorporates both dynamical evolution and statistical decay. More specifically, we will show that the experimental charge distributions as well as the main features of the coincident events can be reproduced by coupling a dynamical approach describing the formation of the primary fragments, to a statistical stage where these excited primary fragments can undergo any division from particle evaporation to symmetric fission.

The dynamic stage of the collision was simulated by solving the Boltzmann-Nordheim-Vlasov (BNV) equation. The resulting average trajectory in phase space, is followed up to a time called for the sake of convenience, the "relaxation" time. We have chosen the relaxation time as the time when the slope of the emitted nucleon mean energy curve changes, indicating the transition from preequilibrium emission to evaporation from a more equilibrated source.

At the relaxation time, a clustering procedure[12] is used to calculate, for each impact parameter, the primary fragment observables: mass, charge, velocity, angle, excitation energy and angular momentum. In this procedure a cluster is formed by the test particles that satisfy the relation $|r_i-r_j|<D$, where D is set to the minimum value that reproduces the mass of the target and projectile at t = 0 (D = 1.5 fm). With this method we obtain the most probable distribution of primary fragments with all their properties at the relaxation time as a function of impact parameter.

Finally, these sources are allowed to undergo sequential binary decays. The deexcitation process has been simulated with the statistical decay code GEMINI[5]. In this code, all decay channels are considered, from light particle emission to symmetric division.

The model described above has been applied to the reaction $^{139}La + ^{27}Al$ at 55 MeV/u[3]. For the most central impact parameters (b = 1, 2 fm), the BNV calculations predict the occurrence of fusion accompanied by preequilibrium emission. For b = 3 fm, the mechanism observed can be characterized as fast fission. Finally the more peripheral reactions lead to a process whose features are very reminiscent of deep inelastic collisions

as they are observed at low incident energy. At each impact parameter, preequilibrium emission of light particles is observed. Fig. 5 shows the cross section as a function of atomic number Z for the system under study. Good agreement is observed between the data and the simulation.

More severe constraints are imposed by the coincidence events. Coincident events have been separated according to the detected fragment multiplicity. A n-fold event is defined as an event where n fragments with $Z \geq 4$ are detected. We have compared the branching ratios for the binary, ternary and quaternary channels obtained from the data and the calculation after filtering through the detector acceptance. In both cases, 2-fold events represent the bulk of the detected fragments, and the branching ratios for 3-fold events agree within 20%.

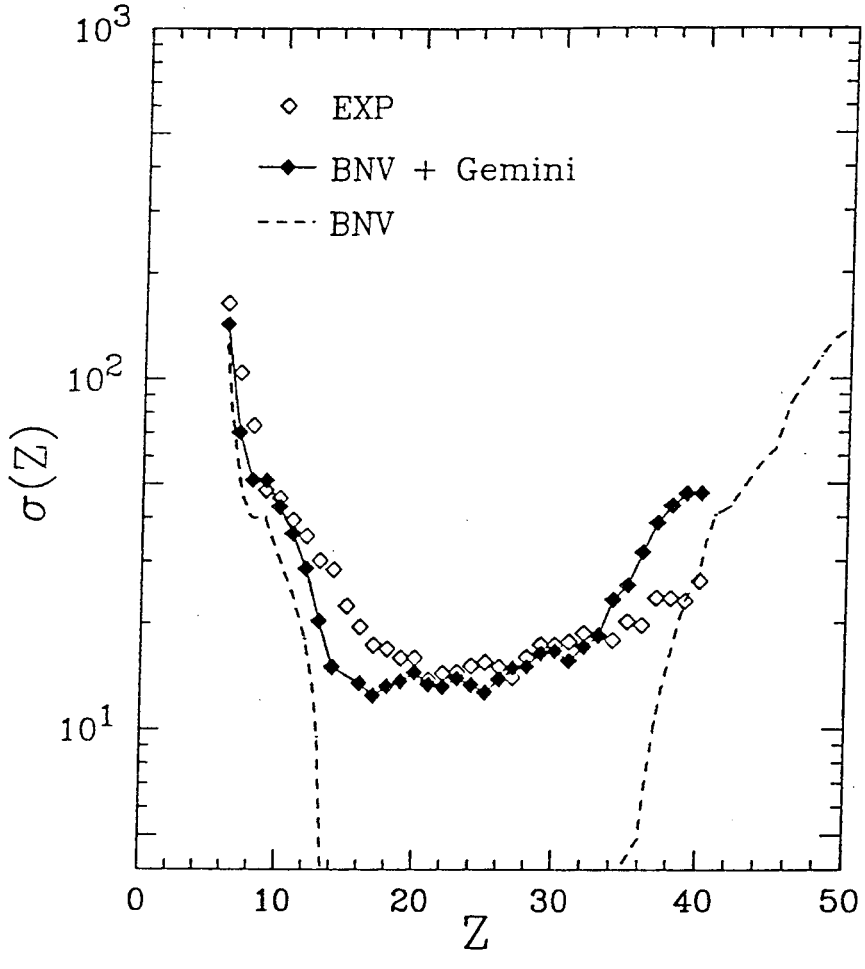

Fig.5 : Comparison of the experimental and calculated charge distribution for the system La + Al at 55 MeV/u. No normalization factor has been applied to the simulation. The statistical errors on experimental data are smaller than the diamonds and the errors related to the extraction procedure are smaller than 20% except above Z = 35 where the cross section can be underestimated by up to 60% due to the reduced angular coverage for the very heavy fragments.

The experimental total charge and source velocity distributions with the corresponding theoretical quantities obtained from the calculations after filtering through our detection efficiency, are shown in Fig. 6. The overall agreement is satisfactory. The peak position in the Z_{tot} distribution for the 2-fold events is well reproduced. For the 3-fold events, the peak position obtained in the calculation is somewhat larger than the data. The shift observed in the Z_{tot} peak position may also be due to an underestimate of the excitation energy deposited in the primary sources. The source velocity distributions (shown Fig. 6) are gated for $Z_{tot} \geq 30$, in order to reduce to a reasonable level the contamination arising from incompletely detected events and to avoid biasing our kinematical reconstructions. For all types of events, the position of the calculated peak is in good agreement with the data, but the width is underestimated for 3 and 4-fold events.

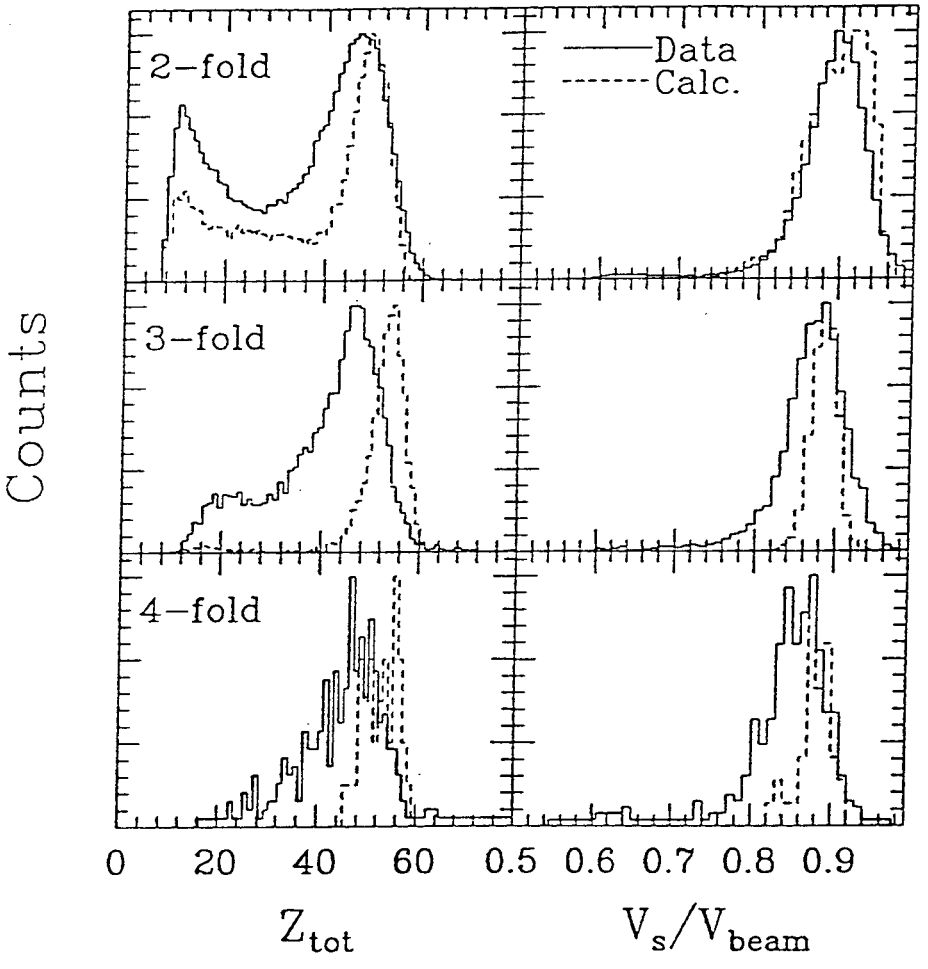

Fig. 6 : Comparison of the experimental (solid line) and calculated (dashed line) total charge (left-hand column) and source velocity (right-hand column) distributions for different fragment multiplicities in the case of $^{139}La + ^{27}Al$ at 55 MeV/u. The spectra have been normalized to the same maximum.

The 3-body decay features are best shown by means of Dalitz plots. In the Dalitz plots presented here, a gate has been applied to the total detected charge (Z_{tot}>30). Fig. 7 compares the data with the results of the "BNV+Gemini" calculation before and after filtering. It should be stressed that at the end of the dynamical stage the Dalitz plot would be empty, since either an incomplete fusion residue or a target and projectile remnant are produced. After the deexcitation stage, the simulated Dalitz plot is very similar to the data, with a predominance of events with one heavy and two light fragments. The relative abundance of these events located in the corners of the triangle is considerably reduced after filtering through our detection efficiency, because the heavy fragments are strongly forward peaked and very often do not pass through the filter.

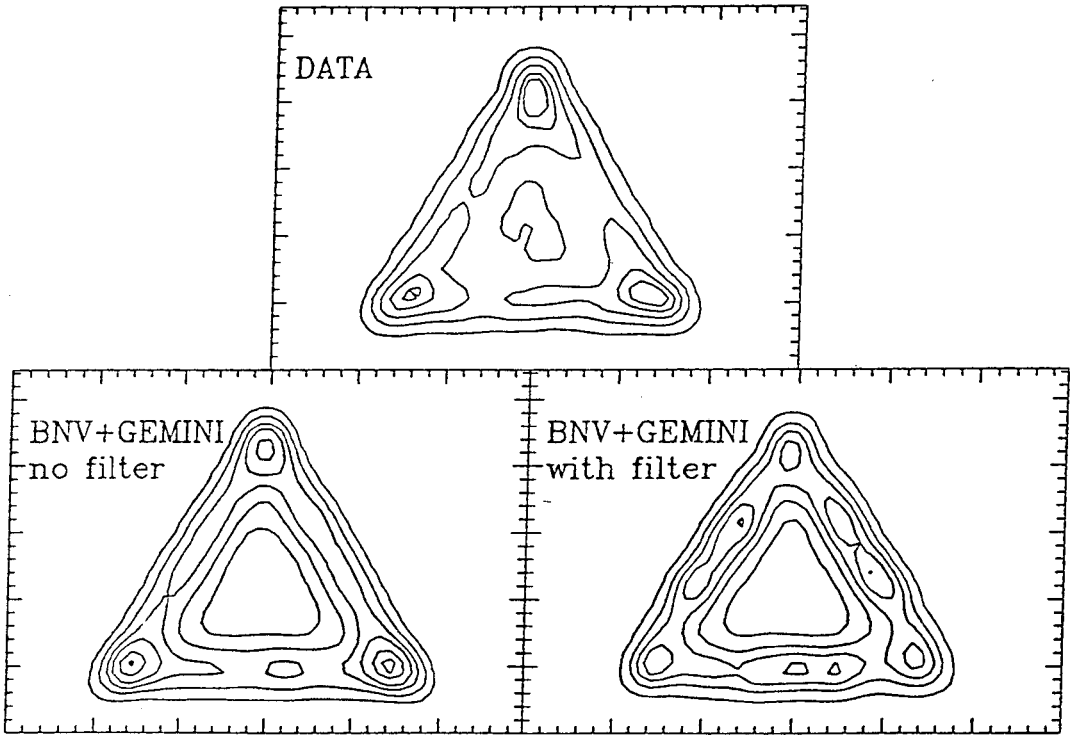

Fig. 7: Comparison of the linear contour Dalitz plots obtained from the data and from the simulation before and after filtering through the detection efficiency, for the system $^{139}La + ^{27}Al$ at 55 MeV/u.

Neutron Calorimeter

Experiments as those described above, would greatly benefit from the knowledge of the neutron multiplicity associated with each event. This would allow one to gate on the highest energy deposition events, and to verify the validity of extracting the Q value kinematically.

So far two main techniques of neutron multiplicity measurements have been developed, the first based on multidetector walls or balls, the second on the thermalization

of neutrons and the counting of the capture events which are dispersed in time (Gd-doped liquid balls). For high multiplicities of fast neutrons, these techniques suffer from a large cross talk between the detectors due to the increased path of multiple scattered neutrons, or from the difficulty of thermalizing high energy neutrons in a reasonable volume of scintillating liquid. In addition, the Gd balls are very slow because of the thermalization and capture time of about 100 μs.

We have developed a technique [15] particularly adapted to high energy neutrons and higher multiplicities. The response function of a plastic scintillation detector to a neutron is distributed up to the maximum light yield of the protons recoils, even if a sufficient depth of scintillating material is provided to allow for the slowing down of the incoming neutron. Even if this response were to be, as a worst case completely flat, and it is not, the integral response to a number ν_n of monoenergetic neutrons detected at the same time has a mean value equal to ν_n times the mean response to a single neutron, and a dispersion approximately $\sqrt{\nu_n}$ times the dispersion for a single neutron. If the neutron multiplicity ν_n is sufficiently high, a reasonably low relative dispersion can be obtained, with a mean response proportional to the multiplicity. Thus, high multiplicities of neutrons of approximately the same energy can be measured through the total light response of a plastic scintillator calorimeter to the neutrons. The requirement of a low neutron energy spread is fulfilled with reverse kinematics reactions where the source velocities can be made much greater than the mean neutron velocity in the source frame.

A standard neutron scintillator program has been modified to accumulate the response of many neutron histories and, in addition, to propagate the neutrons also in inert materials, as the ones of the shielding. The calculated response functions, for $\nu_n = 30$, have dispersions between ±15% and ±19% depending upon the neutron energy.

Acknowledgements

This work was supported by the Director, Office of Energy Research, Division of Nuclear Physics of the Office of High Energy and Nuclear Physics of the US Department of Energy under contract DE-AC03-76SF00098.

References

[1] N. Colonna et al., *Phys. Rev. Lett.* **62**, 1833 (1989)
[2] Y. Blumenfeld et al., *Phys. Rev. Lett.* **66**, 576 (1991)
[3] P. Roussel-Chomaz et al., in preparation
[4] A. Bonasera et al., *Phys. Lett.* **B244**, 169 (1990)
[5] R.J. Charity et al., *Nucl. Phys.* **A483**, 371 (1988)
[6] R.J. Charity et al., *Nucl. Phys.* **A476**, 516 (1988)
[7] R. Bougault et al., *Phys. Lett.* **B232**, 291 (1989)
[8] Ch. Gregoire et al., Nucl. Phys. **A465**, 315 (1987)
[9] H. Stöcker and W. Greiner, *Phys. Rep.* **137**, 277 (1986)
[10] G.F. Bertsch and S. Das Gupta, *Phys. Rep.* **160** (1988) 190 and references therein
[11] A. Bonasera, G.F. Burgio, M. Di Toro, *Phys. Lett.* **B221**, 233 (1989)
A. Bonasera, G. Russo, H.H. Wolter, *Phys. Lett.* **B246**, 337 (1990)
[12] A. Bonasera et al., *Phys. Lett.* **B244**, 169 (1990)
[13] A. Adorno et al., *Nucl. Phys.* A in press
[14] D.R. Bowman et al., *Nucl. Phys.* **A523**, 386 (1991)
[15] A. Pantaleo et al., *Nucl. Instr. & Meth.* **A269**, 580 (1988)

LAWRENCE BERKELEY LABORATORY
UNIVERSITY OF CALIFORNIA
INFORMATION RESOURCES DEPARTMENT
BERKELEY, CALIFORNIA 94720